ASN NEURO RESEARCH ARTICLE

Sex-specific activation of cell death signalling pathways in cerebellar granule neurons exposed to oxygen glucose deprivation followed by reoxygenation

Jaswinder Sharma*,†, Geetha Nelluru*, Mary Ann Wilson*,†,‡, Michael V Johnston*,†,§ and Mir Ahamed Hossain*,†1

*Hugo W. Moser Research Institute at Kennedy Krieger, Baltimore, MD 21205, U.S.A.
†Department of Neurology, Johns Hopkins University School of Medicine, Baltimore, MD 21205, U.S.A.
‡Department of Neuroscience, Johns Hopkins University School of Medicine, Baltimore, MD 21205, U.S.A.
§Department of Pediatrics, Johns Hopkins University School of Medicine, Baltimore, MD 21205, U.S.A.

ABSTRACT

Neuronal death pathways following hypoxia–ischaemia are sexually dimorphic, but the underlying mechanisms are unclear. We examined cell death mechanisms during OGD (oxygen-glucose deprivation) followed by Reox (reoxygenation) in segregated male (XY) and female (XX) mouse primary CGNs (cerebellar granule neurons) that are WT (wild-type) or Parp-1 [poly(ADP-ribose) polymerase 1] KO (knockout). Exposure of CGNs to OGD (1.5 h)/Reox (7 h) caused cell death in XY and XX neurons, but cell death during Reox was greater in XX neurons. ATP levels were significantly lower after OGD/Reox in WT-XX neurons than in XY neurons; this difference was eliminated in Parp-1 KO-XX neurons. AIF (apoptosis-inducing factor) was released from mitochondria and translocated to the nucleus by 1 h exclusively in WT-XY neurons. In contrast, there was a release of Cyt C (cytochrome C) from mitochondria in WT-XX and Parp-1 KO neurons of both sexes; delayed activation of caspase 3 was observed in the same three groups. Thus deletion of Parp-1 shunted cell death towards caspase 3-dependent apoptosis. Delayed activation of caspase 8 was also observed in all groups after OGD/Reox, but was much greater in XX neurons, and caspase 8 translocated to the nucleus in XX neurons only. Caspase 8 activation may contribute to increased XX neuronal death during Reox, via caspase 3 activation. Thus, OGD/Reox induces death of XY neurons via a PARP-1-AIF-dependent mechanism, but blockade of PARP-1-AIF pathway shifts neuronal death towards a caspase-dependent mechanism. In XX neurons, OGD/Reox caused prolonged depletion of ATP and delayed activation of caspase 8 and caspase 3, culminating in greater cell death during Reox.

Key words: apoptosis, caspase 3, caspase 8, hypoxia–ischaemia, neuronal death, sexual dimorphism.

INTRODUCTION

HI (hypoxia–ischaemia) in the preterm and neonatal brain is a leading cause of neurodevelopmental disabilities and intellectual impairment in surviving infants and children (Johnston, 1997; Lorenz et al., 1998; Northington et al., 2001a, 2001b), for which currently there is no promising therapy. The mechanisms underlying the neuronal cell death in brain after HI are complex, as they depend on multiple factors and appear in a variety of forms (Dirnagl et al., 1999; Vannucci and Hagberg, 2004; Endres et al., 2008). Furthermore, an important new concept is now

emerging that chromosomal sex is an important determinant of the pathophysiology of, and outcome after, acute neuronal injury (Johnston and Hagberg, 2007; Rosamond et al., 2007; Yuan et al., 2009). However, sex differences in brain injury in the paediatric and post-menopausal populations suggest that the effects of reproductive steroids may not completely explain sexual dimorphism in brain injury (Hurn et al., 2005; Vannucci and Hurn, 2009). Sex specificity studies of HI brain injury, both *in vivo* and *in vitro*, studies suggest that mechanisms of ischaemic cell death are not identical between male and female sexed cells (Carruth et al., 2002; Zhang et al., 2003; Du et al., 2004; Renolleau et al., 2008), supporting the notion that divergent pathways of cell death occur between chromosomal sexes (Hall et al., 1991; Nunez et al., 2001). Yet, the chromosomal sex-based relationship between the extent of the cellular and biochemical events occurring following HI, other than hormonal influences, is not completely understood (Watanabe et al., 2009).

The developing brain is highly susceptible to damage by HI that affects the cellular and systemic substrates, reduced ATP supply, abnormal gene regulation and production of cellular free radicals resulting in neuronal injury (McDonald et al., 1988; Choi and Rothman, 1990; Barks and Silverstein, 1992; Martin et al., 1997; Johnston, 2001). Various *in vivo* and *in vitro* studies of HI brain injury have shown that apoptotic cell death may occur via caspase-independent pathways that involve AIF (apoptosis-inducing factor) or via caspase-dependent pathways (Yu et al., 2003; Wang et al., 2004; Zhu et al., 2006). In addition, the extrinsic cell death pathway is driven by activation of plasma membrane death receptors and caspase 8, and that both pathways converge on the downstream caspase 3 (Cohen, 1997; Li et al., 1998). Previously, we observed that *Parp-1* gene disruption in mice preferentially protected males over females from neonatal brain injury (Hagberg et al., 2004). Sex specificity has also been demonstrated in cell culture models; after cytotoxic exposure, apoptosis in cortical neurons proceeded predominantly via an AIF-dependent pathway in male (XY) neurons versus a Cyt C (cytochrome c)-dependent pathway in female (XX) neurons (Susin et al., 1999; Yu et al., 2003; Du et al., 2004; Wang et al., 2004; Zhu et al., 2006). These basic cell death pathways show dramatic sexual dimorphism, suggesting mechanisms that may underlie the differences in outcome of brain injury (Golomb et al., 2008). Here, we used segregated XY and XX primary cerebellar granule neuronal cultures that are either WT (wild-type) or *Parp-1* KO, modelled *in vitro* using transient OGD (oxygen-glucose deprivation), to examine sex-related differences in the activation of both intrinsic- and extrinsic-cell death pathways. CGNs (cerebellar granule neurons) are most suitable for analysing molecular mechanisms of cell death differences between chromosomal sexes because of their abundance and homogeneity. Our results show that there are sex differences in the process of initiating mitochondrial-mediated cell death between male and female, and suggest that sex-specific impairment of mitochondrial activity and apoptotic changes account for the enhanced levels of vulnerability of XX neurons compared with XY neurons during the OGD–Reox (reoxygenation) phase.

MATERIALS AND METHODS

Parp-1 gene–deficient mice

The Johns Hopkins University Institutional Animal Care and Use Committee approved all animal protocols used; they complied with the U.S. National Institutes of Health approved Guide for the Care and Use of Laboratory Animals. The *Parp-1*-KO mice used in these studies have a disruption at the second exon of the *Parp-1* gene (Wang et al., 1995). *Parp-1*-KO mice generated on an SV129 background were backcrossed with CD-1 mice to obtain F5 CD-1 ($\sim$97%)/SV-129 ($\sim$3%) mice. *Parp-1* heterozygous mice were then bred to obtain litters consisting of WT, KO and heterozygous offspring. Male and female mice were identified on postnatal day 3 to 4 by visual inspection and a tail sample obtained for *Parp-1* genotyping.

Genotyping using PCR

Genomic DNA was isolated from tail samples following the method as described by Conner (2002). Briefly, the tail was digested with 0.5 ml of 0.05 M NaOH and incubated for 10–20 min at 95℃ and then neutralized by adding 50 µl of a solution of 1 M Tris/HCl, 10 mM EDTA (pH 8.0). Three microlitres were used directly in a 22-µl PCR reaction. The WT-*Parp-1* and *Parp-1*-KO allele was amplified using a common primer (5′-ACAGCATCAGGCAGCCTCTGTT-3′) and primers specific for the intact *Parp-1* alleles were (5′-CTTGACCTTCTGCTGATCATCC-3′) or the inserted Neo cassette (5′-GATGCTCTTCGTCCAGATCATCC-3′). PCR was performed in a DNA thermal cycler (Peltier thermal cycler, PTC-200, MJ Research, Waltham, MA, U.S.A.); denaturation was for 5 min at 95℃ followed by 29 cycles of denaturation at 95℃ for 45 s, annealing at 60℃ for 45 s, extension at 72℃ for 1 min and a final extension at 72℃ for 5 min. The reaction products were separated by 2% agarose gel electrophoresis and visualized with ethidium bromide under UV illumination. Appropriate controls for WT and *Parp-1*-KO were included on each gel. The genotypes were identified by single DNA bands of 231 bp (WT, homozygous), single $\sim$600 bp *Parp-1*-KO (homozygous) or two DNA bands of 231 and 600 (heterozygous).

Sex-segregated cerebellar granule neuronal cultures from WT and *Parp-1* gene–deficient mice

Primary cultures of CGNs were isolated from P7 male and female mice that were either WT or *Parp-1*-KO, segregated based on sex and PARP-1 genotype, according to methods described previously (Hossain et al., 2002). Cells were resuspended in a medium consisting of 10% FBS (Gemini Bioproducts, Calabasas, CA, U.S.A.), 25 mM KCl, 100 µg/ml primocin (Invivogen, San Diego, CA, U.S.A.) and 2 mM L-glutamax (Invitrogen, Carlsbad, CA, U.S.A.) in Basal Medium Eagle (Life Technologies, Rockville, MD, U.S.A.) and were

seeded at a density of 2.5×10^5 cells/cm^2 area in multi-well plates or in dishes (Corning, Corning, NY, U.S.A.) precoated with poly-L-lysine (100 µg/ml; Sigma, St Louis, MO, U.S.A.). The cells were maintained for DIV 9 (9 days *in vitro*) at 37℃ in the presence of 5% CO$_2$/95% air in a humidified incubator. Cytosine arabinofuranoside (AraC, 5 µM; Sigma) was added to cultures 24 h after plating to arrest the growth of non-neuronal cells. With this protocol, >95% of the cultured cells were MAP-2 (microtubule-associated protein-2) immunoreactive neurons (Chemicon, Temecula, CA, U.S.A.) (Dudek et al., 1997; Hossain et al., 2002).

Induction of OGD

OGD was initiated at DIV 9 cultures by replacing culture medium with deoxygenated, glucose-free extracellular solution (140 mM NaCl, 25 mM KCl, 1.3 mM CaCl$_2$, 0.8 mM MgCl$_2$ and 10 mM Hepes). In the control cells, the culture medium was replaced with control solution (140 mM NaCl, 25 mM KCl, 5.5 mM glucose, 1.3 mM CaCl$_2$, 0.8 mM MgCl$_2$ and 10 mM Hepes). KCl was included in the medium (25 mM) to ensure normal neuronal development and survival in cultures and to minimize neuronal death from causes other than OGD/Reox (D'Mello et al., 1993; Hossain et al., 2002). Hypoxia was induced by exposing cells to humidified 95% N$_2$/5% CO$_2$ at 37℃ using a modular incubator chamber (Billups-Rothenberg, Del Mar, CA, U.S.A.) as described previously (Hossain et al., 2004). After indicated periods of exposure, cells were returned to control normoxic medium containing glucose and incubated for additional 7 h. Control cultures were exposed to humidified 95% air/5% CO$_2$ at 37℃.

Assessment of cell viability: calcein AM (acetoxymethyl ester)/PI (propidium iodide) uptake

At the end of OGD (1.5 h)/Reox (7 h) treatment, cultures were washed thrice with HBSS (Hanks' balanced salt solution; 144 mM NaCl, 10 mM Hepes, 2 mM CaCl$_2$, 1 mM MgCl$_2$, 25 mM KCl and 10 mM glucose, pH 7.4). Cells were incubated at 37℃ in fresh HBSS containing 0.1 µM of calcein AM (Invitrogen) and 0.5 µM of PI for 15 min. Calcein AM, a non-fluorescent hydrophobic compound easily permeates intact live cells. The hydrolysis of Calcein AM by intracellular esterases produces calcein, a hydrophilic, strongly fluorescent compound that is well retained in the cytoplasm of viable cells. Cell injury curtails calcein staining and allows for cell permeation with PI, a polar compound that by interacting with nuclear DNA, yields a bright red fluorescence (Amoroso et al., 1997). Following calcein AM/PI treatment, cultures were washed with HBSS, and images were collected within 10–15 min with an inverted fluorescence microscope (Olympus 1 × 51 equipped with DP2-DSW-V3.2 application software) using appropriate colour filters. Cell death was quantified by PI/calcein and expressed as a percentage of the total number of cells counted.

Assessment of cell cytotoxicity: LDH (lactate dehydrogenase) assay

LDH released into the media after OGD (1.5 h) and OGD (1.5 h)/Reox (7 h) exposure was measured using the Cytotoxicity Detection Kit (LDH) (Roche Diagnostics Corporation, Indianapolis, IN, U.S.A.) as described previously (Hossain et al., 2004). Percentage cell death was determined using the formula: % cytotoxicity OGD/Reox LDH release (A_{490})/maximum LDH release (A_{490}) after correcting for baseline absorbance (A) of LDH release at 490 nm.

TUNEL (terminal deoxynucleotidyl transferase-mediated dUTP nick–end labelling) staining

The Dead End Fluorometric TUNEL System (Promega, Madison, WI, U.S.A.) was used to detect OGD (1.5 h) and OGD (1.5 h)/Reox (7 h)-induced cell death in cultured CGNs as described previously (Hossain et al., 2004). This method allows direct detection of nuclear DNA fragmentation, an important biochemical hallmark of cell death, by catalytically incorporating fluorescein-12-dUTP at 3′-OH DNA ends. Negative controls were performed under identical conditions except for the omission of terminal deoxynucleotidyl transferase from the reaction buffer provided with the TUNEL kit. Fluorescence was visualized in a fluorescence microscope (Carl Zeiss Axioplan 1) with an λ_{ex} at 485 nm and an λ_{em} at 535 nm and DAPI (4′,6-diamidino-2-phenylindole) fluorescence (blue) was visualized with an λ_{ex} and λ_{em} filters at 365 nm and 450 nm respectively.

Immunofluorescence

Immunofluorescence staining of primary CGN cells, grown on coverslips, was conducted essentially as described previously (Russell et al., 2006). Specific antibodies used were: rabbit monoclonal cleaved caspase 3 (Cell Signaling, Beverly, MA, U.S.A.), mouse monoclonal (clone 6H2.B4), Cyt C (BD Biosciences Pharmingen, San Diego, CA, U.S.A.) and rabbit polyclonal AIF (Cell Signaling). The mitochondrial-specific markers used were ATP β synthase (Chemicon International, Tamecula, CA, U.S.A.) and VDAC (voltage-dependent anion channel; Abcam, Cambridge, MA, U.S.A.). For Cyt C-specific immunostaining, neurons were also subjected to antigen retrieval using 5% urea in 0.1 M Tris/HCl at 95℃ for 10 min. Briefly, CGNs at DIV 9 were fixed with 3.7% formaldehyde and permeabilized cells were double labelled with AIF (1:100) and ATP synthase (1:300) antibodies, Cyt C (1:100) and VDAC (1:300), and cleaved caspase 3 (1:200) for overnight at 4℃ according to our previously described method (Russell et al., 2006). For negative controls, appropriate non-immune IgG was used instead of primary antibodies. Cells were washed and stained with donkey anti-mouse and anti-rabbit (1:300) Alexa fluor-conjugated secondary antibodies (Invitrogen) for 1 h at room temperature (21℃). Slides were coverslipped with prolong mounting medium containing DAPI (blue) (Molecular Probes, Eugene, OR, U.S.A.) to stain nuclei. Immunofluorescence was visualized

using a fluorescence microscope (Carl Zeiss Axioplan 1 microscope fitted with AxioVision 3.0 software) at ×40 and confocal microscope (Olympus Fluoview) using the FV 1000 confocal system at ×100 magnification as described previously (Hossain et al., 2004; Russell et al., 2006).

Subcellular fractionation

Subcellular fractionation was performed as described previously (Russell et al., 2008). Briefly, cells were harvested in ice-cold PBS and centrifuged at 3600 **g** for 5 min. Cell pellets were resuspended in isotonic MB (mitochondrial buffer) consisting of 210 mM mannitol, 70 mM sucrose, 1 mM EDTA and 10 mM Hepes, pH 7.5, supplemented with protease and phosphatase inhibitor cocktails (Calbiochem, San Diego, CA, U.S.A.). Cells were homogenized with a Dounce homogenizer for 20 strokes and were centrifuged at 500 **g** for 5 min (Wang et al., 2004). The pellet is the nuclear fraction and was resuspended in 30–50 µl of MB with 0.1% Triton X-100. The post-nuclear supernatant was centrifuged further at 10000 **g** for 30 min at 4°C for the mitochondrial fraction. The pellet containing the mitochondrial fraction was suspended in 50 µl of MB containing 0.1% Triton X-100 to break up the mitochondria; the supernatant was used as the crude cytosolic fraction. To confirm the separation of cytosolic, mitochondrial and nuclear fractions, blots were stripped and incubated with actin, prohibitin and histone respectively, which also served as a loading control.

SDS/PAGE and Western–blot analyses

SDS/PAGE and immunoblotting were performed according to the method as described previously (Hossain et al., 2002). Briefly, CGN extracts were prepared using 50 µl of ice-cold lysis buffer RIPA (PBS 1×, 1% Igepal CA-630, 0.5% sodium deoxycholate, 0.1% SDS) containing 1× protease cocktail inhibitor set 1 (Calbiochem), sodium vanadate (1 mM), sodium pyrophosphate (2 mM) and sodium β-glycerophosphate (1 mM) and stored at −70°C. Total proteins (10–20 µg), measured by the bicinchoninic protein assay (Pierce, Rockford, IL, U.S.A.), were diluted in Laemmli buffer containing 2-mercaptoethanol, heated to 100°C for 5 min, separated on a 4–20% gradient Tris-glycine precast gel (Invitrogen) at 120 V for 1.5 h, and then immunoblotted with primary antibodies for procaspase-3 and cleaved caspase 3 (1:1000; Cell Signaling), AIF (1:1000; Cell Signaling), Cyt C (1:1000; BD Biosciences, clone 7H8.2C12), caspase 8 (1:1000; Cell Signaling), histone H3 (1:1000, rabbit monoclonal; Cell Signaling), prohibitin (1:1000 rabbit polyclonal; Abcam) and actin (1:5000, mouse monoclonal anti β-actin antibody; Sigma, St Louis, MO, U.S.A.). HRP (horseradish peroxidase)-conjugated secondary antibodies (GE Healthcare, Piscataway, NJ, U.S.A.) were used at 1:5000 dilutions for 1 h at room temperature. The HRP (horseradish peroxidase) reaction product was then visualized by ECL® (enhanced chemiluminescence) using an ECL Western blotting detection kit (GE healthcare). Digitized images were quantified using ImageJ software.

Caspase 3 activity assay

DEVDase caspase 3-like activity was measured using colorimetric assay kit CASPASE-3 Cellular Activity Assay Kit PLUS (Biomol, Plymouth Meeting, PA, U.S.A.) according to the manufacturer's instructions. The release of free pNA (p-nitroaniline) from colorimetric substrate N-acetyl-Asp-Glu-Val-Asp-pNA was monitored colorimetrically at 405 nm for 1 h using a multi-well microtitre plate reader (Spectra MAX 340pc; Molecular Devices, Sunnyvale, CA, U.S.A.). Caspase 3 activity was measured as nmol of pNA released/min per mg of protein and expressed as a percentage of control.

Caspase 8 activity assay

The Caspase 8 Colorimetric Assay Kit (Biomol) was used to estimate the caspase 8 activity according to the manufacturer's instructions. The release of free pNA was monitored colorimetrically at 405 nm for 1 h using a multi-well microtitre plate reader (Spectra MAX 340pc; Molecular Devices). Caspase 8 activity was measured as nmol of pNA released/min per mg of protein and expressed as a percentage of control.

Measurements of cellular ATP

Intracellular ATP levels were determined by using ATPlite, a luminescence-based kit (PerkinElmer, Waltham, MA, U.S.A.). Cellular extracts were prepared from DIV-9 CGN cells seeded on 24 well plates and exposed to OGD and OGD/Reox as indicated. Cells were collected adding an appropriate volume of mammalian lysis buffer. ATP quantification in the extracts was performed according to the manufacturer's instructions. Chemiluminescence was measured in luminometer (Tristar LB 941, Berthold Technologies, Oak Ridge, TN, U.S.A.). Results were normalized according to the protein content of the extracts.

Statistical analysis

Statistics were performed using the StatView 5.0 program. Comparisons involving multiple groups were done by ANOVA, followed by Bonferroni/Dunn post-hoc test where appropriate. Significance level was assigned at $P < 0.05$.

RESULTS

Sex-specific vulnerability to neuronal death in response to OGD followed by Reox, *in vitro*

CGNs incubated under normoxic conditions were healthy and retained normal morphology, as indicated by large size, phase brightness and intact processes (Figure 1A). There were no obvious gross morphological differences between XY and XX or WT and PARP-1-KO CGNs under normoxic conditions. However, light microscopic analyses of CGNs following OGD

(1.5 h)/ Reox (7 h) showed characteristic morphological changes: the neurons were round, smaller and translucent, with disintegration of processes. Sex-specific neuronal death was quantitatively analysed by an LDH release cytotoxicity assay (Figure 1B). Exposure to 1.5 h of OGD resulted in 20–25% LDH release compared with normoxia controls. However, exposure to OGD (1.5 h)/Reox (7 h) resulted in significantly more cell death in WT-XX CGNs (LDH release 62%; ** $P<0.01$) compared with WT-XY (46%). Deletion of the *Parp-1* gene was not protective in XX CGNs (67% in KO-XX, comparable with that observed in WT-XX 62%), but provided significant protection in XY CGNs (38% in KO-XY, *$P<0.05$ compared with 46% in WT-XY). Thus, in this model, there are marked differences in vulnerability to OGD/Reox in XX and XY CGNs, and deletion of the *Parp-1* gene provides sex-specific neuroprotection against OGD/Reox in XY CGNs (KO-XY) only. This protection in male PARP-1-KO neurons but not in female neurons is consistent with previous observations *in vivo* after neonatal HI (Hagberg et al., 2004) and adult ischaemia (McCullough et al., 2005). Next, DNA fragmentation after OGD (1.5 h)/Reox (7 h) was examined using TUNEL staining (Figure 1C). Exposure to OGD/ Reox led to significantly increased number of TUNEL-(+) cells in WT and *Parp-1*-KO-XY and -XX CGNs compared with control normoxia cells ([+++]$P<0.001$). Quantification of TUNEL (+) cells showed significantly increased DNA fragmentation in WT-XX neurons after 7 h of Reox compared with that observed with WT-XY neurons (*$P<0.05$). Interestingly, a significantly higher number of TUNEL (+) cells was observed in KO-XX neurons (**$P<0.01$) compared with that in KO-XY (Figure 1C).

Assessment of cell viability using calcein/PI

We employed calcein/PI fluorescence incorporation as a measure of cell viability between XX and XY neurons. OGD (1.5 h)/Reox (7 h) led to reduced cellular viability in WT-XX
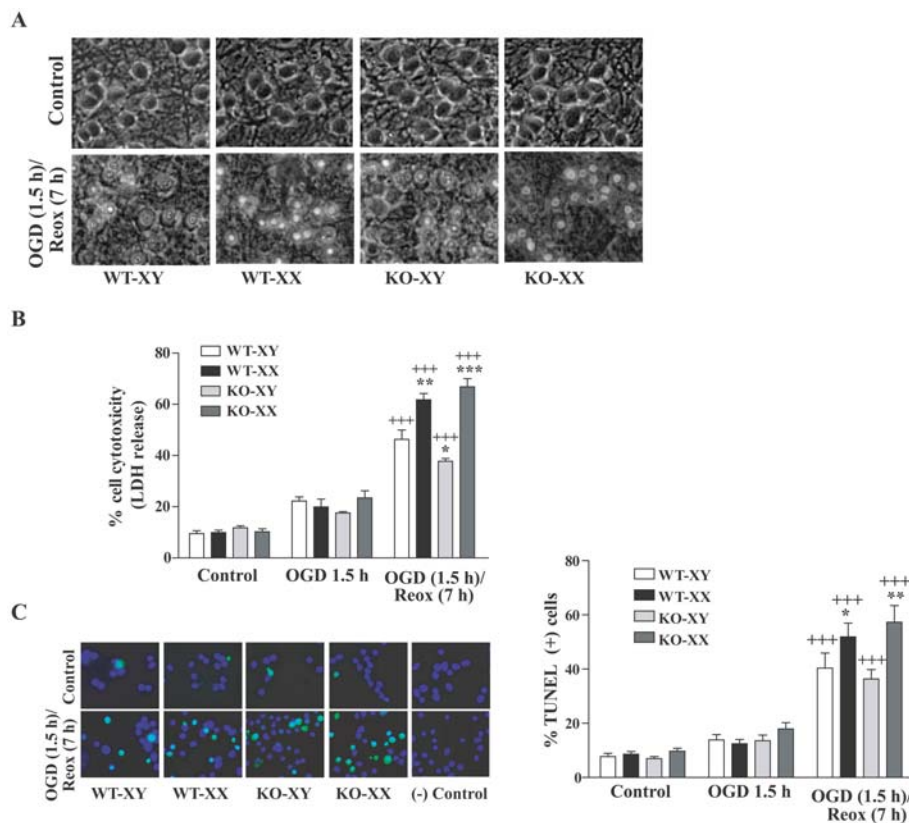

Figure 1   Sex-related differences in OGD– and OGD/Reox-induced neuronal death
The cells were exposed to OGD for 1.5 h or to 1.5 h OGD followed by 7 h of Reox. (**A**) Morphological evidence of injury in WT- and *Parp-1*-KO-XX CGNs as compared with that in WT- and KO-XY neurons. A higher magnitude of cell injury was observed in both WT- and KO-XX CGNs. The *Parp-1*-KO-XY neurons exhibited lesser extent of injury than that in WT-XY CGNs. (**B**) Quantification of cell death by LDH release also revealed significantly higher percentage of cell death in female as compared with male CGNs after 7 h Reox following 1.5 h of OGD. Values are means ± S.E.M. ($n=4$), **$P<0.01$, WT-XX versus WT-XY; ***$P<0.001$, KO-XX versus KO-XY, and [+++]$P<0.001$ versus control. (**C**) Fluorometric TUNEL immunostaining (green) of CGNs exposed to OGD (1.5 h)/Reox (7 h) showed enhanced fluorescence of TUNEL (+) cells in XX cells of both WT and KO genotype as compared with WT-XY and KO-XY CGN cells. Quantification of TUNEL-(+) cells revealed significantly higher cell death in WT- and KO-XX than in WT-XY and KO-XY CGNs (means ± S.E.M.; $n=4$,*$P<0.05$ WT-XX versus WT-XY, **$P<0.01$ KO-XX versus KO-XY, [+++]$P<0.001$ versus control).

(*P<0.05) and KO-XX (***P<0.001) CGNs as indicated by marked loss of calcein fluorescence (green) with concomitant increase in PI (red) fluorescence compared with that in WT- and KO-XY CGNs respectively (Figure 2A).

Sex difference in cellular ATP utilization following OGD/Reox

To evaluate changes in neuronal bioenergetic status after OGD (1.5 h) or OGD (1.5 h)/Reox (7 h), we measured cellular ATP levels in XY and XX CGNs. Total cellular ATP levels were significantly decreased following OGD (1.5 h) with partial recovery following Reox (7 h). However, ATP content was markedly more decreased in the WT-XX neurons as compared with WT-XY neurons, declining to only ~15% of control levels after 1.5 h of OGD and reaching levels of approx. 38% of basal after Reox (***P<0.001). These striking differences in ATP content suggest that impaired energy metabolism may contribute to the increased vulnerability of WT-XX neurons to OGD/Reox-induced death. ATP content in KO-XX CGNs was comparable with that in WT- and KO-XY CGNs, suggesting that PARP-1 activation during OGD/Reox may have contributed to the increased ATP depletion in WT-XX neurons (Figure 2B).

Sex difference in mitochondrial release of AIF in CGNs following OGD

We examined the cellular distribution of the apoptosis inducing factor AIF, a caspase-independent death regulator, to evaluate possible sex differences in mitochondrial AIF release in response to OGD. Cells were double immunostained with AIF (red) and mitochondrial-specific marker ATP synthase (green) and nuclei were stained with DAPI as described in the Materials and methods. Confocal microscopy in control (normoxic) conditions revealed mitochondrial co-localization of AIF and ATP synthase (yellow), with no AIF localized in the nucleus (blue) (Figure 3A). After 30 min exposure to OGD, AIF-specific immunofluorescence was no longer restricted to mitochondria in XY CGNs, but was localized in the cytoplasm (red), primarily in the perinuclear region. After 1 h of OGD, nuclear translocation (purple) was apparent in XY CGNs. In contrast, AIF-specific fluorescence in XX CGN cells under identical exposure remained co-localized with ATP synthase (intense yellow) for up to 1 h of OGD exposure, indicating that AIF was retained within mitochondria in XX CGNs. However, after prolonged exposure to OGD (2 h), a small amount of AIF release (red) was detected in XX CGNs and some nuclear localization was observed. These results clearly
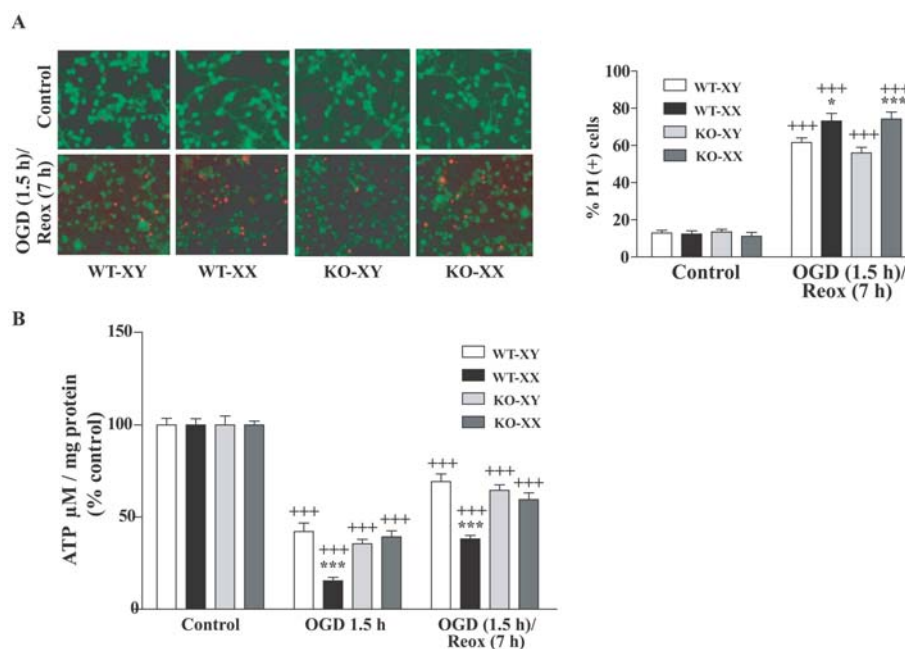

Figure 2   Effects of OGD (1.5 h) or OGD (1.5 h) followed by Reox (7 h) on neuronal viability and cellular ATP content in CGNs
(A) Neuronal survival and death was assessed using the fluorescent dyes calcein AM (green) and PI (red) incorporation following exposures. Control normoxia cells were viable as evident by intense calcein-specific green fluorescence (upper panel). Increased red fluorescence intensity of PI indicates enhanced cell death following OGD/Reox (lower panel). Quantification of calcein- and PI- (+) cells revealed a significantly higher percentage of cell death in WT-XX (73%) and KO-XX (74%) than in WT-XY (62%) and KO-XY (56%) respectively. Results are means±S.E.M. (n=4, *P<0.05 WT-XX versus WT-XY and ***P<0.001 KO-XX versus KO-XY, +++P<0.001 versus control). (B) Exposure to OGD (1.5 h) or to OGD (1.5 h)/Reox (7 h) resulted in significant reduction in ATP content with much greater and prolonged reduction observed in WT-XX neurons than in WT- and KO-XY neurons. ATP concentration was assayed as described in the Materials and methods. Data were expressed as percentage of control (100%) and shown as means±S.E.M. for at least three separate experiments (***P<0.001, WT-XX versus WT-XY; +++P<0.001 versus control).

show that AIF release and nuclear translocation occurring more rapidly in XY neurons than in XX neurons in response to OGD exposure. AIF release and translocation were not observed in KO CGNs, which appeared similar to normoxic cells (results not shown).

To confirm and quantify the sex-dependent release and translocation of AIF in CGNs and the effects of *Parp-1* gene deletion, we evaluated OGD exposed CGNs by cell fractionation, separating mitochondrial and nuclear fractions and analysing them by Western blotting. In the mitochondrial fraction of control normoxic CGNs, an intense AIF-immunoreactive band was detected at 67 kDa (Figure 3B). Following exposure to OGD (1 h), there was a significant decrease in AIF protein in the mitochondrial fraction from WT-XY compared with WT-XX CGNs (*$P<0.05$) with a simultaneous increase in AIF protein in the nuclear fraction of WT-XY (**$P<0.01$ versus WT-XX; $^{+++}$ $P<0.001$ versus control normoxia). There was no significant increase in WT-XX CGNs or in KO CGN of either sex (Figure 3C).

Early release of Cyt C from mitochondria into the cytoplasm in XX CGNs following OGD

To investigate the sex-specific differences in the intrinsic Cyt C-dependent pathway of apoptotic cell death, we determined the time course of Cyt C release from mitochondria in XY and XX CGNs following OGD exposure. Double immunofluorescence labelling of CGNs was performed to examine the subcellular localization of Cyt C (red) and the mitochondrial marker VDAC (green). Confocal microscopic ($\times 100$) analysis detected that Cyt C-specific immunofluorescence (red) was entirely overlapped with mitochondrial marker VDAC (shown as yellow in Figure 4A) in both control XY and XX cells, confirming mitochondrial localization of Cyt C under normoxic conditions. In WT CGNs exposed to OGD, we found Cyt C release at 30 min in XX neurons, with more pronounced release observed at 1 h, as evidenced by the appearance of red fluorescence in the cytoplasm. On the other hand, in XY neurons, Cyt C release into the cytoplasm was evident after 1 h or more OGD exposure. Cyt C release was also apparent in
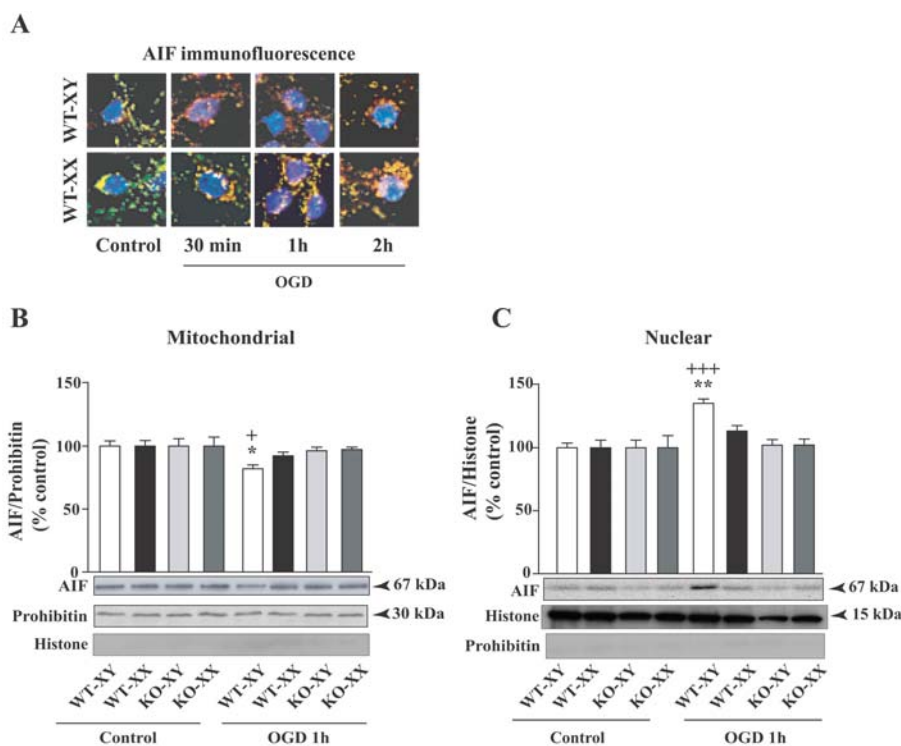

Figure 3 **Mitochondrial release of AIF and nuclear translocation in WT–XY and WT–XX CGNs following OGD exposure**
(**A**) Primary CGNs were immunostained with AIF (red), mitochondrial marker ATP synthase (green); DAPI stained nucleus of cells (blue) and analysed by confocal microscopy. Under normal conditions, AIF and ATP synthase are co-localized in mitochondria (yellow). Exposure at different time periods of OGD showed mitochondrial release of AIF at 30 min in WT–XY cells as AIF-specific immunofluorescence was localized in the perinuclear region of cytoplasm (red) and nuclear localization at 1 h OGD (purple), but remained localized in the mitochondria of WT–XX neurons under identical conditions. No AIF or ATP synthase-specific immunofluorescence was observed in cells incubated with non-immune IgG (negative controls). (**B**) AIF translocation was also assessed by subcellular fractionations and Western-blot analyses. Quantification of AIF-specific protein band showed significant decrease in AIF protein levels in the mitochondrial fraction from WT–XY CGNs with concomitant increase in the nuclear fraction of WT–XY CGNs in comparison with WT–XX cells (**C**). Values represent means $\pm$ S.E.M. ($n=4$) ($^+P<0.05$, $^{+++}P<0.001$ versus control normoxia cells; *$P<0.05$, **$P<0.01$ WT–XY versus WT–XX). *Parp-1*-KO-XY and -XX CGNs retained AIF within the mitochondria under similar exposure. Prohibitin and histone were used as a control for purity of the mitochondrial and nuclear fraction respectively, which also served as loading controls. Representative blots are shown.

Parp-1-KO CGNs (XY and XX) exposed to OGD, although the release appeared less pronounced (results not shown).

To confirm Cyt C release, we performed subcellular fractionations and Western immunoblot analyses of mitochondrial and cytoplasmic fractions that showed an intense Cyt C-specific protein band (15 kDa) in the control mitochondrial fraction from both XX and XY cells. After 1 h OGD, a modest decrease in the Cyt C-specific protein band was observed in the mitochondrial fraction (Figure 4B) with a concomitant increase in the cytosolic fraction of WT XX and PARP-1-KO neurons of both sexes (+++$P<0.001$, + $P<0.05$ versus control) but not in WT-XY neurons (Figure 4C). This increase in cytosolic Cyt C in WT-XX was also significantly higher (*$P<0.05$) compared with WT-XY CGNs.

Sex differences in caspase 3 activation following OGD/Reox

Mitochondrial release of Cyt C, procaspase-3 proteolysis/activation and oligonucleosomal DNA fragmentation are the

phenotypic hallmarks of caspase-mediated apoptosis (Budd et al., 2000). Here, we examined the effects of sex differences on caspase 3 activation in response to OGD (1.5 h) and OGD (1.5 h)/Reox (7 h). A colorimetric assay using the caspase 3-specific substrate Ac-DEVD-pNA (*N*-acetyl-Asp-Glu-Val-Asp-7-pNA; 200 µM) was used to detect caspase 3 activity in the whole cell lysates by monitoring the cleavage and release of free pNA (Figure 5A). Caspase 3-like activity was not changed after 1.5 h OGD, but when exposed to OGD followed by 7 h of Reox, WT-XX CGNs exhibited a significant increase in caspase 3-like activity compared with WT-XY cells (247% versus 134%, respectively; ***$P<0.001$). The pancaspase inhibitor Ac-DEVD-CHO (*N*-acetyl-Asp-Glu-Val-Asp aldehyde; 0.1 µM) completely inhibited the caspase 3-like activity (Figure 5A), suggesting the specificity of the caspase activation assay. Interestingly, an increase in caspase 3-like activity (Figure 5A) was also seen in *Parp-1*-KO-XY and -XX CGN cells (188% and 217 ± 4.1% respectively; **$P<0.01$ versus WT-XY CGNs). Our results indicate an increased flux through the caspase-dependent pathway in the absence of
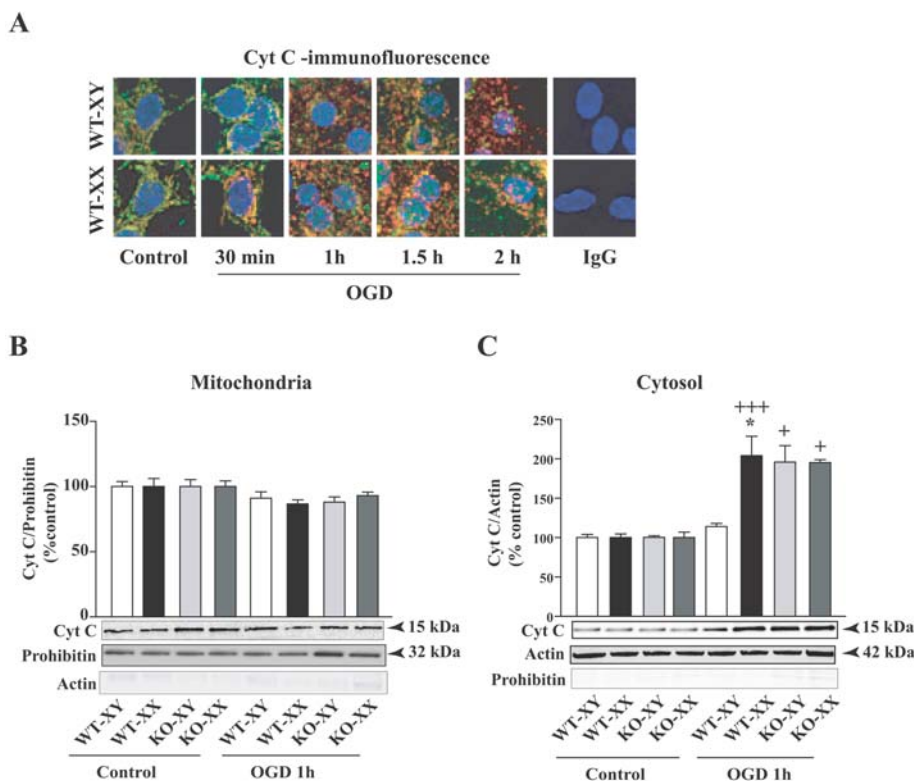

Figure 4   **Mitochondrial release of Cyt C in XY and XX CGNs following OGD exposure**
(**A**) Primary CGNs were immunostained with Cyt C (red), mitochondrial marker VDAC (green); DAPI-stained nucleus of cells (blue). Confocal microscopy of double immunofluorescence staining with Cyt C and VDAC and merged images (yellow) detected Cyt C predominantly localized within the mitochondrial compartment of control CGN cells. OGD exposure resulted in Cyt C release from mitochondria into the cytoplasmic region (red) within 30 min OGD onset and more pronounced release at 1 h in WT-XX cells in comparison with WT-XY neurons. No Cyt C- or VDAC-specific immunofluorescence was observed in cells incubated with non-immune IgG (negative controls). (**B**) Subcellular fractionation and quantification of the Cyt C-specific protein band showed OGD-dependent decrease in Cyt C protein levels in the mitochondrial fraction with simultaneous increase in the cytoplasmic fraction of WT-XX and KO-XX CGNs (**C**). Unlike AIF, Cyt C release was also observed in *Parp-1*-KO-XY cells than in WT-XY neurons. Values represent means ± S.E.M. ($n=4$; *$P<0.05$ WT-XX versus WT-XY. +++$P<0.001$, +$P<0.05$ versus controls). Prohibitin and actin were used as a control for purity of the mitochondrial and cytosolic fraction respectively, which also serve as loading controls. Representative blots are shown.

PARP-1 in males (*Parp-1*-KO-XY CGNs). Next, Western-blot analysis using an antibody that detects the activated (cleaved) form of caspase 3 showed cleaved caspase 3-specific immunoreactive protein bands (17 and 19 kDa, normalized to procaspase-3 protein at 35 kDa) that were significantly increased in WT-XX cells, but not in WT-XY cells, following OGD/Reox (***$P<0.001$ versus WT-XY; [++] $P<0.001$ versus controls) (Figure 5B). Most interestingly, cleaved caspase 3 protein was significantly increased in *Parp-1*-KO-XY and -XX cells compared with WT-XY (**$P<0.01$ and *$P<0.05$ respectively), confirming the activation of caspase 3 activity (Figure 5A). To further confirm the sex-specific differential activation of caspase 3, we performed immunocytochemical analysis of cleaved caspase 3 under similar conditions, and

counted the number of cleaved caspase 3 (+) cells. Control normoxic cells from both sexes and genotype showed almost no or very smaller number of cleaved caspase 3 (+) positive cells. A marked increase in the number of cleaved caspase 3 (+) cells was seen in both WT and KO of XY and XX cells after OGD (1.5 h)/Reox (7 h), compared with controls ([++]$P<0.001$); however, the increase in cleaved-caspase 3 (positive) cells was significantly higher in WT-XX neurons (*$P<0.05$) compared with that in WT-XY neurons (Figure 5C).

Caspase 8 activation in females

Caspase 8 is the prototypic initiator of the so-called extrinsic death receptor pathway of apoptosis (Boldin et al., 1996;
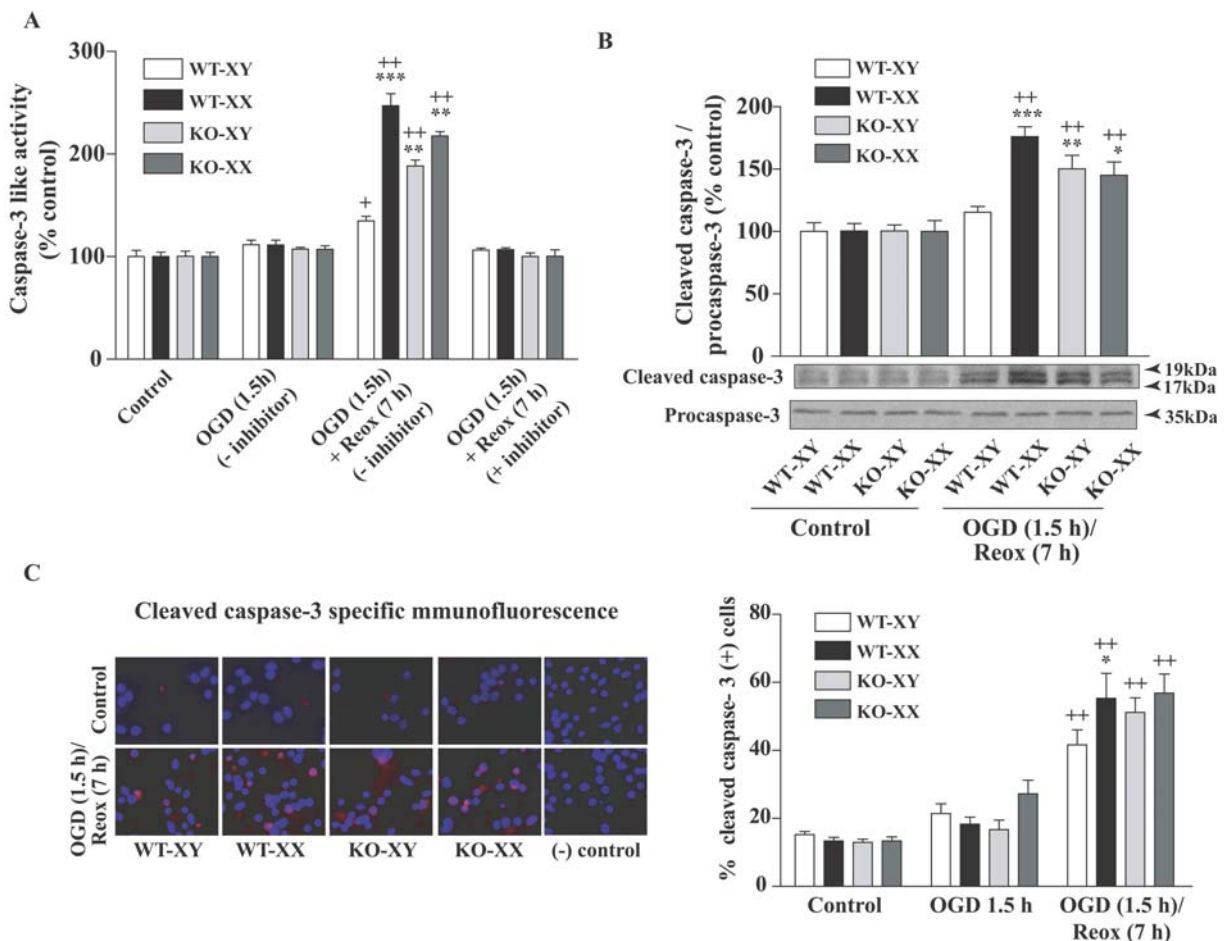

Figure 5   **Sex–specific activation of caspase 3 in CGNs exposed to OGD (1.5 h) or OGD (1.5 h) followed by Reox (7 h)**
(**A**) Caspase 3-like activity assay from total cellular extract showed no change in caspase 3 activity after 1.5 h OGD, but caspase 3 activity was significantly increased in WT-XX CGNs following Reox (7 h) in comparison with WT-XY cells. Interestingly, an increase in caspase 3-like activity was also seen in *Parp-1*-KO-XX and KO-XY CGN cells. Results are means ± S.E.M. (*n*=3; ***$P<0.001$ WT-XX versus WT-XY, **$P<0.01$ KO-XY and KO-XX versus WT-XY CGNs; [+]$P<0.05$, [++]$P<0.001$ versus normoxic control). (**B**) Western immunoblot using cleaved caspase 3-specific antibody detected increased cleaved caspase 3 protein band in WT-XX CGNs and in CGNs from *Parp-1*-KO genotype of either sex. Values are normalized to procaspase-3 and expressed as a percentage of control (100%) (means ± S.E.M., *n*=3; ***$P<0.001$, **$P<0.01$ and *$P<0.05$ in comparison with WT-XY; [++]$P<0.001$ in comparison with normoxic control). Representative blots are shown. (**C**) Caspase 3-specific immunostaining and quantification of caspase 3 (+) cells at 7 h Reox following 1.5 h of OGD showed similar increase in cleaved caspase 3 (+) cells, which paralleled the increased caspase 3-like activity (**A**). Cleaved caspase 3 (+) cells at 1.5 h of OGD were not significantly different from normoxic control cells (results not shown). Values are means ± S.E.M. (*n*=3, *$P<0.05$ WT-XX versus WT-XY; [++]$P<0.001$ versus normoxic control cells).

Benchoua et al., 2002). To elucidate the possible mechanisms that could be involved in greater vulnerability to OGD/Reox-induced neuronal damage in females, we assessed caspase 8 activation to evaluate the extrinsic pathway. A colorimetric assay using the caspase 8-specific substrate IETD-pNA (200 µM) was used and the release of free pNA was monitored to determine the proteolytic activity of caspase 8 (Figure 6A). No activation of caspase 8-like activity was observed at earlier time period of OGD (1.5 h). Whole cell lysates from WT- and KO-XX exhibited a significantly greater increase (~3 fold; **$P<0.01$ and *$P<0.05$ respectively) in peptide cleavage activity following OGD (1.5 h)/Reox (7 h) than in WT- and KO-XY cells, suggesting sex specificity in caspase 8 activation in the XX neurons. Caspase 8 has distinct cytoplasmic and nuclear roles and can act as an executioner at nuclear levels in the process of ischaemic-apoptotic neuronal death (Benchoua et al., 2002). To further confirm the participation of caspase 8, we examined caspase 8 nuclear localization following OGD/Reox by subcellular fractionation and Western blotting of nuclear fraction (Figure 6B). Quantification of cleaved caspase 8 protein bands (~45 kDa) normalized to full-length caspase 8 (57 kDa) showed significantly greater amount of cleaved caspase 8 protein in WT- and KO-XX CGNs compared with normoxic controls (++$P<0.001$) or in comparison with WT- and KO-XY neurons (***$P<0.001$) (Figure 6B). Together these results provide evidence of sex differences in caspase 8 activation and suggest that the presence of active caspase 8 in the nucleus of XX neurons may contribute to the greater magnitude of cell death in XX neurons following OGD/Reox.

DISCUSSION

The present study provides strong evidence of sex differences in neuronal injury in segregated XY and XX primary CGNs at the Reox phase after a period of OGD exposure. First, OGD triggered mitochondrial release of AIF, a major triggering event for large-scale DNA fragmentation and neuronal death, at a much earlier time in XY neurons than in XX neurons. In contrast, cell death in XX neurons proceeded with more pronounced release of Cyt C from mitochondria into the cytoplasm. There was depletion of cellular ATP content following OGD/Reox, and this depletion was much more severe in the XX neurons than in XY neurons, suggesting an increased vulnerability of XX neurons to death (Eguchi et al., 1997). Secondly, significantly higher levels of caspase 3 activation in XX neurons during the Reox phase caused a greater magnitude of cell death in XX neurons than in the XY neurons, as evidenced by a significantly higher percentage of LDH release, TUNEL staining and calcein/PI dye fluorescent staining in XX cells during the Reox phase. Most interestingly, caspase 3 activation was also observed in *Parp-1*-KO cells of both sexes. Thirdly, the XX neurons of both WT
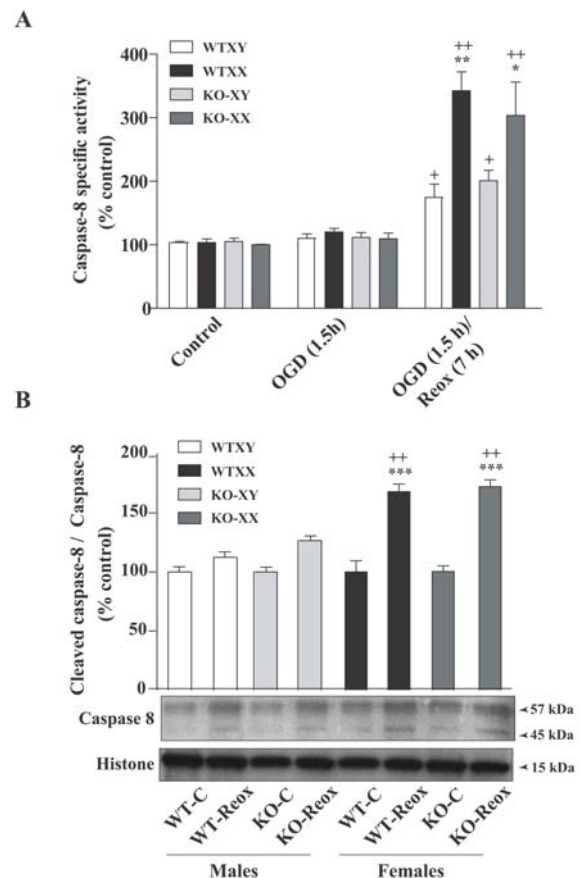

Figure 6 Sex–specific activation of caspase 8 in CGNs exposed to OGD (1.5 h) or OGD (1.5 h) followed by Reox (7 h)
(**A**) Results showed increased caspase 8-specific peptide cleavage activity following 7 h of Reox in WT- and KO-XX cells only, but not in WT- and KO-XY CGNs. Results are means ± S.E.M., $n=3$ (**$P<0.01$, *$P<0.05$ in comparison with both WT- and KO-XY neurons respectively; +$P<0.05$, ++$P<0.001$ versus control). (**B**) Cellular extracts were subjected to fractionation after the indicated time of exposure, and the nuclear fraction was analysed by Western-blot analysis for the full-length (57 kDa) and the cleaved form (45 kDa). Quantification of cleaved active fragments of caspase 8 (normalized to 57 kDa bands) showed significant increase of cleaved caspase 8 at 7 h Reox in WT- and *Parp-1*-KO-XX cells only. Results are expressed as a percentage of control (100%) (means ± S.E.M., $n=3$, ***$P<0.001$ in comparison with both WT- and KO-XY neurons, ++$P<0.001$ in comparison with control). Representative blots are shown.

and *Parp-1*-KO genotype, in contrast with XY neurons, exhibited significantly greater increased activation and nuclear translocation of caspase 8 following OGD/Reox. Most importantly, in contrast with caspase 3 activation, the nuclear localization of caspase 8 occurred in the XX neurons only, which may be responsible for the higher magnitude of XX neuronal death. Together, our results clearly demonstrate the sex specificity in the timing of mitochondrial release of death-initiating factors AIF and Cyt C, and the differential responses of the intrinsic and extrinsic cell death pathways could account for the higher magnitude of neuronal death in XX than in XY neuronal cells during the Reox period after OGD.

Emerging evidence suggests that sex differences exist in the 'sensitivity' of male and female brain to specific molecular signalling pathways engaged by cerebral HI (Lang and McCullough, 2008; Cheng and Hurn, 2010). Our findings in cell culture model are in agreement with previous reports that, after cytotoxic challenge, apoptosis proceeded predominantly via an AIF-dependent pathway in XY neurons versus a Cyt C-dependent pathway in XX neurons (Du et al., 2004; Hagberg et al., 2004), suggesting that cell death pathways differ innately according to sex (Penaloza et al., 2009). Several previous studies by others (Arnold et al., 2004; Du et al., 2004; Renolleau et al., 2008; Penaloza et al., 2009) and the present study shows that cell death can be the result of the genetic complement of cells according to the sex, yet do not discount the importance of sex steroids and hormones (McCullough et al., 2001; McCullough and Hurn, 2003; Hurn et al., 2005; Vannucci and Hurn, 2009). In our experimental model, the depletion of ATP content during the OGD-Reox phase is consistent with the findings of others (Scorziello et al., 2001; Serra-Perez et al., 2008), but there was a much greater reduction of cellular ATP content in XX neurons than in XY neurons. This could lead to mitochondrial dysfunction in XX neurons, resulting in Cyt C release and massive plasma membrane damage (LDH release). All these events together may result in a higher magnitude of cell death in XX CGNs than in XY CGNs. By contrast, Li et al. (2005) reported intrinsic neuroprotection in the female-derived hippocampal slice cultures but not in the male cultures in response to OGD or NMDA (N-methyl-D-aspartate) exposure. However, in this study, we found a paradoxical effect in that female sex does not offer any advantage against OGD-Reox induced neuronal death. Cell death in certain brain regions can be different in both magnitude and duration between male and female (Nunez et al., 2001), thus emphasizing the importance of regionally specific sex differences in the apoptotic death pathways irrespective of differences in available sex steroids. In addition, developmentally regulated cell death was observed greater in the primary visual cortex of developing females than in males during the formation of sex difference in adult neurons (Nunez et al., 2001). Thus, the observed discrepancy is possibly the result of the more active and prolonged apoptotic programme in the developing cerebellum than in the post-mitotic hippocampal slice cultures. Furthermore, variations in culture conditions, brain tissue slice versus more homogeneous primary neuronal cultures, may exist that may also account for the differential response in sex-specific neuronal death. Increased cell death in female sex has also been reported in many instances; XX cortical neurons were found to be more susceptible to apoptotic cell death induced by etoposide and staurosporine than XY neurons (Du et al., 2004). Hilton et al. (2003) showed that females, rather than males, were more sensitive to kainic acid-induced hippocampal damage in rat pups, and female cells being significantly more sensitive to stressors such as ethanol- and camptothecin-induced cell death than male cells (Penaloza et al., 2009), documenting the sex-dimorphic cell

response to death. Similarly, female cortical astrocytes sustained greater cell death than males when inflammatory mediators were combined with OGD (Liu et al., 2007; Cheng and Hurn, 2010). All these studies attribute a persistent pattern of more cell death in females than males, which are congruent with our findings.

To date, the best studied sex-specific mechanisms involves a set of molecules that lead to neuronal apoptosis; caspase-independent PARP-1-AIF death pathway that is highly engaged in male ischaemic brain (Susin et al., 1999; Daugas et al., 2000; Wang et al., 2009) and caspase-dependent neuronal death pathway culminating in more apoptosis in females (Du et al., 2004; Renolleau et al., 2008). We found that AIF was released at an earlier time point and translocated to the nucleus in WT-XY neurons following OGD but not in WT-XX neurons. On the other hand, the late activation of caspase 3 and caspase 8 probably contributed to the delayed but higher magnitude of XX cell death during the Reox phase. Interestingly, increased caspase 3 activation was also observed in *Parp-1*-KO-XY neurons similar to KO-XX neurons. Activation of caspase 3 was reported in transplanted PARP$^{-/-}$ dopaminergic neuron in nigral grafts (Schierle et al., 1999), and PARP$^{-/-}$ skin fibroblast cells displayed substantially more caspase 3 activity than PARP$^{+/+}$ cells following toxic insult (Rosenthal et al., 2001). Thus, it appears that loss of PARP-1 shunted the cells towards another detrimental pathway of caspase 3 activation, which in turn accounts for the observed cell death in *Parp-1*-KO neurons. However, the cell death in *Parp-1*-KO-XY CGNs was significantly less than in the WT-XY cells, suggesting neuroprotection in the PARP-1 KO state of XY neurons during the OGD-Reox phase.

Another important aspect of this study is the striking sex differences observed in the activation and nuclear localization of caspase 8 in XX neurons (both WT and *Parp-1*-KO) compared with XY neurons during Reox after OGD. Caspase 8 has distinct cytoplasmic and nuclear roles, and is the primary activator of the extrinsic death receptor pathways of apoptosis (Sanchez et al., 1999; Benchoua et al., 2002). Caspase 8 activates caspase 3 and can also translocate to the nucleus where it targets nuclear protein of the PARP family, PARP-2 (Benchoua et al., 2002), which, like PARP-1, is also involved in the maintenance of genomic integrity and cell survival (Ame et al., 1999). In addition, caspase 8 can also induce apoptotic cell death through the mitochondrial pathway by cleaving the cytoplasmic factor Bid, a pro-apoptotic member of the Bcl-2 protein family (Li et al., 1998). The role of caspase 8 and its nuclear translocation in sex-specific cell death following OGD/reperfusion is not completely understood. Our findings of increased caspase 8 activation and high levels of its nuclear localization in the XX cells could only lead to an exacerbation of neuronal death, and this may be an important regulatory mechanism of apoptosis during the Reox period in females.

In conclusion, our results show that XX neurons are more sensitive to OGD/Reox-induced neuronal injury compared with XY CGNs. Our results identify potentially important mechanistic differences in cell death between XY and XX

neurons under OGD-Reox periods. It appears that AIF and caspase 8 play specific roles in determining sex differences in neuronal death. Results presented here clearly demonstrate sexual dimorphic nature between male and female neuronal cell death during the Reox phase following an OGD episode, and provide insights towards therapeutic strategies at post-HI stage based on chromosomal sex.

REFERENCES

Ame JC, Rolli V, Schreiber V, Niedergang C, Apiou F, Decker P, Muller S, Hoger T, Menissier-de Murcia J, de Murcia G (1999) PARP-2, A novel mammalian DNA damage-dependent poly (ADP-ribose) polymerase. J Biol Chem 274:17860–17868.

Amoroso S, De Maio M, Russo GM, Catalano A, Bassi A, Montagnani S, Renzo GD, Annunziato L (1997) Pharmacological evidence that the activation of the Na(+)-Ca^{2+} exchanger protects C6 glioma cells during chemical hypoxia. Br J Pharmacol 121:303–309.

Arnold AP, Xu J, Grisham W, Chen X, Kim YH, Itoh Y (2004) Minireview: sex chromosomes and brain sexual differentiation. Endocrinology 145:1057–1062.

Barks JD, Silverstein FS (1992) Excitatory amino acids contribute to the pathogenesis of perinatal hypoxic-ischemic brain injury. Brain Pathol 2:235–243.

Benchoua A, Couriaud C, Guegan C, Tartier L, Couvert P, Friocourt G, Chelly J, Menissier-de Murcia J, Onteniente B (2002) Active caspase-8 translocates into the nucleus of apoptotic cells to inactivate poly (ADP-ribose) polymerase-2. J Biol Chem 277:34217–34222.

Boldin MP, Goncharov TM, Goltsev YV, Wallach D (1996) Involvement of MACH, a novel MORT1/FADD-interacting protease, in Fas/APO-1- and TNF receptor-induced cell death. Cell 85:803–815.

Budd SL, Tenneti L, Lishnak T, Lipton SA (2000) Mitochondrial and extramitochondrial apoptotic signaling pathways in cerebrocortical neurons. Proc Natl Acad Sci USA 97:6161–6166.

Carruth LL, Reisert I, Arnold AP (2002) Sex chromosome genes directly affect brain sexual differentiation. Nat Neurosci 5:933–934.

Cheng J, Hurn PD (2010) Sex shapes experimental ischemic brain injury. Steroids 75:754–759.

Choi DW, Rothman SW (1990) The role of glutamate neurotoxicity in hypoxic-ischemic neuronal death. Annu Rev Neurosci 13:171–182.

Cohen GM (1997) Caspases: the executioners of apoptosis. Biochem J 326:1–16.

Conner DA (2002) Mouse colony management. Curr Protoc Mol Biol 23:8.1–8.11.

D'Mello SR, Galli C, Ciotti T, Calissano P (1993) Induction of apoptosis in cerebellar granule neurons by low potassium: inhibition of death by insulin-like growth factor I and cAMP. Proc Natl Acad Sci USA 90:10989–10993.

Daugas E, Nochy D, Ravagnan L, Loeffler M, Susin SA, Zamzami N, Kroemer G (2000) Apoptosis-inducing factor (AIF): a ubiquitous mitochondrial oxidoreductase involved in apoptosis. FEBS Lett 476:118–123.

Dirnagl U, Iadecola C, Moskowitz MA (1999) Pathobiology of ischaemic stroke: an integrated view. Trends Neurosci 22:391–397.

Du L, Bayir H, Lai Y, Zhang X, Kochanek PM, Watkins SC, Graham SH, Clark RS (2004) Innate gender-based proclivity in response to cytotoxicity and programmed cell death pathway. J Biol Chem 279:38563–38570.

Dudek H, Datta SR, Franke TF, Birnbaum MJ, Yao R, Cooper GM, Segal RA, Kaplan DR, Greenberg ME (1997) Regulation of neuronal survival by the serine-threonine protein kinase Akt. Science 275:661–665.

Eguchi Y, Shimizu S, Tsujimoto Y (1997) Intracellular ATP levels determine cell death fate by apoptosis or necrosis. Cancer Res 57:1835–1840.

Endres M, Dirnagl U, Moskowitz MA (2008) Chapter 2 The ischemic cascade and mediators of ischemic injury. Handb Clin Neurol 92:31–41.

Golomb MR, Garg BP, Saha C, Azzouz F, Williams LS (2008) Cerebral palsy after perinatal arterial ischemic stroke. J Child Neurol 23:279–286.

Hagberg H, Wilson MA, Matsushita H, Zhu C, Lange M, Gustavsson M, Poitras MF, Dawson TM, Dawson VL, Northington F, Johnston MV (2004) PARP-1 gene disruption in mice preferentially protects males from perinatal brain injury. J Neurochem 90:1068–1075.

Hall ED, Pazara KE, Linseman KL (1991) Sex differences in postischemic neuronal necrosis in gerbils. J Cereb Blood Flow Metab 11:292–298.

Hilton GD, Nunez JL, McCarthy MM (2003) Sex differences in response to kainic acid and estradiol in the hippocampus of newborn rats. Neuroscience 116:383–391.

Hossain MA, Bailone JC, Gomez R, Laterra J (2002) Neuroprotection by scatter factor/hepatocyte growth factor and FGF-1 in cerebellar granule neurons is phosphatidylinositol 3-kinase/Akt-dependent and MAPK/CREB-independent. J Neurochem 81:365–378.

Hossain MA, Russell JC, O'Brien R, Laterra J (2004) Neuronal pentraxin 1: a novel mediator of hypoxic-ischemic injury in neonatal brain. J Neurosci 24:4187–4196.

Hurn PD, Vannucci SJ, Hagberg H (2005) Adult or perinatal brain injury: does sex matter? Stroke 36:193–195.

Johnston MV (1997) Hypoxic and ischemic disorders of infants and children. Lecture for 38th Meeting of the Japanese Society of Child Neurology, Tokyo, Japan, July 1996. Brain Dev 19:235–239.

Johnston MV (2001) Excitotoxicity in neonatal hypoxia. Ment Retard Dev Disabil Res Rev 7:229–234.

Johnston MV, Hagberg H (2007) Sex and the pathogenesis of cerebral palsy. Dev Med Child Neurol 49:74–78.

Lang JT, McCullough LD (2008) Pathways to ischemic neuronal cell death: are sex differences relevant? J Transl Med 6:33.

Li H, Zhu H, Xu CJ, Yuan J (1998) Cleavage of BID by caspase 8 mediates the mitochondrial damage in the Fas pathway of apoptosis. Cell 94:491–501.

Li H, Pin S, Zeng Z, Wang MM, Andreasson KA, McCullough LD (2005) Sex differences in cell death. Ann Neurol 58:317–321.

Liu M, Hurn PD, Roselli CE, Alkayed NJ (2007) Role of P450 aromatase in sex-specific astrocytic cell death. J Cereb Blood Flow Metab 27:135–141.

Lorenz JM, Wooliever DE, Jetton JR, Paneth N (1998) A quantitative review of mortality and developmental disability in extremely premature newborns. Arch Pediatr Adolesc Med 152:425–435.

Martin LJ, Brambrink A, Koehler RC, Traystman RJ (1997) Primary sensory and forebrain motor systems in the newborn brain are preferentially damaged by hypoxia-ischemia. J Comp Neurol 377:262–285.

McCullough LD, Hurn PD (2003) Estrogen and ischemic neuroprotection: an integrated view. Trends Endocrinol Metab 14:228–235.

McCullough LD, Alkayed NJ, Traystman RJ, Williams MJ, Hurn PD (2001) Postischemic estrogen reduces hypoperfusion and secondary ischemia after experimental stroke. Stroke 32:796–802.

McCullough LD, Zeng Z, Blizzard KK, Debchoudhury I, Hurn PD (2005) Ischemic nitric oxide and poly (ADP-ribose) polymerase-1 in cerebral ischemia: male toxicity, female protection. J Cereb Blood Flow Metab 25:502–512.

McDonald JW, Silverstein FS, Johnston MV (1988) Neurotoxicity of N-methyl-D-aspartate is markedly enhanced in developing rat central nervous system. Brain Res 459:200–203.

Northington FJ, Ferriero DM, Martin LJ (2001a) Neurodegeneration in the thalamus following neonatal hypoxia-ischemia is programmed cell death. Dev Neurosci 23:186–191.

Northington FJ, Ferriero DM, Flock DL, Martin LJ (2001b) Delayed neurodegeneration in neonatal rat thalamus after hypoxia-ischemia is apoptosis. J Neurosci 21:1931–1938.

Nunez JL, Lauschke DM, Juraska JM (2001) Cell death in the development of the posterior cortex in male and female rats. J Comp Neurol 436:32–41.

Penaloza C, Estevez B, Orlanski S, Sikorska M, Walker R, Smith C, Smith B, Lockshin RA, Zakeri Z (2009) Sex of the cell dictates its response: differential gene expression and sensitivity to cell death inducing stress in male and female cells. FASEB J 23:1869–1879.

Renolleau S, Fau S, Charriaut-Marlangue C (2008) Gender-related differences in apoptotic pathways after neonatal cerebral ischemia. Neuroscientist 14:46–52.

Rosamond W, Flegal K, Friday G, Furie K, Go A, Greenlund K, Haase N, Ho M, Howard V, Kissela B, Kittner S, Lloyd-Jones D, McDermott M, Meigs J, Moy C, Nichol G, O'Donnell CJ, Roger V, Rumsfeld J, Sorlie P, Steinberger J, Thom T, Wasserthiel-Smoller S, Hong Y; American Heart Association Statistics Committee and Stroke Statistics Subcommittee (2007) Heart disease and stroke statistics–2007 update: a report from the American Heart Association Statistics Committee and Stroke Statistics Subcommittee. Circulation 115:e69–e171.

Rosenthal DS, Simbulan-Rosenthal CM, Liu WF, Velena A, Anderson D, Benton B, Wang ZQ, Smith W, Ray R, Smulson ME (2001) PARP determines the mode of cell death in skin fibroblasts, but not keratinocytes, exposed to sulfur mustard. J Invest Dermatol 117:1566–1573.

Russell JC, Szuflita N, Khatri R, Laterra J, Hossain MA (2006) Transgenic expression of human FGF-1 protects against hypoxic-ischemic injury in perinatal brain by intervening at caspase-XIAP signaling cascades. Neurobiol Dis 22:677–690.

Russell JC, Whiting H, Szuflita N, Hossain MA (2008) Nuclear translocation of X-linked inhibitor of apoptosis (XIAP) determines cell fate after hypoxia ischemia in neonatal brain. J Neurochem. 106:1357–1370.

Sanchez I, Xu CJ, Juo P, Kakizaka A, Blenis J, Yuan J (1999) Caspase-8 is required for cell death induced by expanded polyglutamine repeats. Neuron 22:623–633.

Schierle GS, Hansson O, Leist M, Nicotera P, Widner H, Brundin P (1999) Caspase inhibition reduces apoptosis and increases survival of nigral transplants. Nat Med 5:97–100.

Scorziello A, Pellegrini C, Forte L, Tortiglione A, Gioielli A, Iossa S, Amoroso S, Tufano R, Di Renzo G, Annunziato L (2001) Differential vulnerability of cortical and cerebellar neurons in primary culture to oxygen glucose deprivation followed by reoxygenation. J Neurosci Res 63:20–26.

Serra-Perez A, Verdaguer E, Planas AM, Santalucia T (2008) Glucose promotes caspase-dependent delayed cell death after a transient episode of oxygen and glucose deprivation in SH-SY5Y cells. J Neurochem 106:1237–1247.

Susin SA, Lorenzo HK, Zamzami N, Marzo I, Snow BE, Brothers GM, Mangion J, Jacotot E, Costantini P, Loeffler M, Larochette N, Goodlett DR, Aebersold R, Siderovski DP, Penninger JM, Kroemer G (1999) Molecular characterization of mitochondrial apoptosis-inducing factor. Nature 397:441–446.

Vannucci SJ, Hagberg H (2004) Hypoxia-ischemia in the immature brain. J Exp Biol 207:3149–3154.

Vannucci SJ, Hurn PD (2009) Gender differences in pediatric stroke: is elevated testosterone a risk factor for boys? Ann Neurol 66:713–714.

Wang H, Yu SW, Koh DW, Lew J, Coombs C, Bowers W, Federoff HJ, Poirier GG, Dawson TM, Dawson VL (2004) Apoptosis-inducing factor substitutes for caspase executioners in NMDA-triggered excitotoxic neuronal death. J Neurosci 24:10963–10973.

Wang Y, Dawson VL, Dawson TM (2009) Poly(ADP-ribose) signals to mitochondrial AIF: a key event in parthanatos. Exp Neurol 218:193–202.

Wang ZQ, Auer B, Stingl L, Berghammer H, Haidacher D, Schweiger M, Wagner EF (1995) Mice lacking ADPRT and poly(ADP-ribosyl)ation develop normally but are susceptible to skin disease. Genes Dev 9:509–520.

Watanabe E, Allen NB, Dostal J, Sama D, Claus EB, Goldstein LB, Lichtman JH (2009) Diagnostic evaluation for patients with ischemic stroke: are there sex differences? Cerebrovasc Dis 27:450–455.

Yu SW, Wang H, Dawson TM, Dawson VL (2003) Poly(ADP-ribose) polymerase-1 and apoptosis inducing factor in neurotoxicity. Neurobiol Dis 14:303–317.

Yuan M, Siegel C, Zeng Z, Li J, Liu F, McCullough LD (2009) Sex differences in the response to activation of the poly (ADP-ribose) polymerase pathway after experimental stroke. Exp Neurol 217:210–218.

Zhang L, Li PP, Feng X, Barker JL, Smith SV, Rubinow DR (2003) Sex-related differences in neuronal cell survival and signaling in rats. Neurosci Lett 337:65–68.

Zhu C, Xu F, Wang X, Shibata M, Uchiyama Y, Blomgren K, Hagberg H (2006) Different apoptotic mechanisms are activated in male and female brains after neonatal hypoxia-ischaemia. J Neurochem 96:1016–1027.